Advanced dynamical risk analysis for monitoring anaerobic digestion process

Jonathan Hess and Olivier Bernard[1]

INRIA (French National Institute of Computer Science and Control), COMORE Research Team, 2004 Route des Lucioles, B.P. 93, 06902 Sophia-Antipolis Cedex, France.

Methanogenic fermentation involves a natural ecosystem that can be used for waste water treatment. This anaerobic process can have two locally stable steady-states and an unstable one making the process hard to handle. The aim of this work is to propose analytical criteria in order to detect hazardous working modes, namely situations where the system evolves towards the acidification of the plant. We first introduce a commonly used simplified model and recall its main properties. In order to assess the evolution of the system we study the phase plane and split it into nineteen zones according to some qualitative properties. Then a methodology is introduced to monitor in real-time the trajectory of the system across these zones and determine its position in the plane. It leads to a dynamical risk index based on the analysis of the transitions from one zone to another, and generates a classification of the zones according to their dangerousness. Finally the proposed strategy is applied to a virtual process based on model ADM1. It is worth noting that the proposed approach do not rely on the value of the parameters and is thus very robust.

1 Introduction and motivation

Anaerobic digestion (AD) is a more and more popular bioprocess (1) that can be used to treat organic wastes (wastewater, solid wastes,...). This complex ecosystem involves more than 140 bacterial species (2) that progressively degrade the organic matter into carbon dioxide (CO_2), biomethane (CH_4) and hydrogen under specific conditions. AD has numerous advantages in comparison to more widespread aerobic techniques. Not only do anaerobic bioprocesses produce less sludge and can treat concentrated substrates but they also produce a renewable energy through the biomethane and the hydrogen. Indeed the biomethane is a highly energetic environmental friendly fuel which can replace natural gas in the perspective of sustainable development. However AD processes are considered to be very delicate to manage since they can become unstable (3) under certain circumstances: disturbances (even small ones) such as an overload or an inhibitor may lead to an accumulation of intermediate compounds (volatile fatty acids) leading potentially to the acidification of the digester. Hence to encourage the use of AD and achieve an optimal recovery of the biogas, dedicated methods that would ensure the process durability must be developed (4).

With this objective numerous authors (5–9) have proposed control algorithms to secure digesters stability both during start-up and steady-state. Renard *et al.* (5) presented a model-based adaptive controller to keep the propionate concentration under an inhibitory threshold. Other authors (7–10) used control strategy based on the response of the process to perturbations (*e.g.* pulses in the feed flow rate) to achieve a fast start-up of a digester or to maintain the organic loading rate (OLR) as high as possible at steady-state.

[1]Corresponding author. Tel.: +33 4 92 38 77 85, fax.: +33 4 92 38 78 58. E-mail addresses: olivier.bernard@inria.fr

However, the process complexity and nonlinearity have sometimes led to disappointing performances of the advanced control strategies on the long term. Moreover, most of the automatic controllers use the OLR as a control action (stirring the dilution rate or the influent concentration), assuming that an additional large storage tank is available, which is rarely realistic at the industrial scale. Hence plant operators often by-pass these automatic controllers, managing the plant manually towards a trade-off between stability and performance.

For the automatic controlled plants as for the manually operated ones, there is a strong need to monitor the process behaviour and assess the process stability and it has been the subject of many studies. Some authors (11, 12) analyse simple models of an anaerobic ecosystem who can exhibit two stable steady-states depending on the operating conditions, one of which being the acidification of the digester. These authors proposed to estimate the domain of attraction of the stable equilibria in order to estimate the risk of going toward the catastrophic situation. The way the attraction domain evolves with the parameters can provide useful guidelines for the design and the management of the plant. On this basis Shen *et al.* (12) present a thorough bifurcation analysis of the system steady-states with respect to the parameter values. Hess and Bernard (11) proposed a static criterion to assess the risk of destabilisation associated to the operating strategy of the plant. The application of this criterion to a real experiment showed that it could predict very early a potential accumulation of volatile fatty acids. However this risk index is independent of the real state of the process, and do not take into account the actual evolution of the system.

The objective of this paper is to analyse and characterise the dynamics of an AD process in order to better assess the risk of going towards process acidification, and thus encourage the energetic recovery of liquid wastes. As an extension of Hess and Bernard (11), here we identify, on the basis of the qualitative analysis of some monitored signals (like the biomethane flow rate) the region of the state space where the system lies, and the associated risk. As a consequence we produce a more accurate risk index of the process stability than in (11), devoted to on-line monitoring of industrial processes. To this end we use theoretical tools that have been developed to describe qualitatively the evolution of nonlinear dynamical systems (13, 14). The approach is based on the analysis of the possible succession of signs of the state variable derivatives. It leads to graphs which represent the possible transitions between the different regions of the state variable space (phase space), and provide hints on the dynamical evolution of the system.

The paper is organised as follows: in the next section we detail the considered dynamical AD model, and the main concepts are introduced. In a first step the model is reduced to a simple two dimensional model and a stability analysis is provided for the case of a bistable system. After pointing up the limits of the static criterion of Hess and Bernard (11), the third part puts the emphasis on the analysis of the model dynamics. This leads to a partitioning of the phase plane. Transition graphs that describe the possible commutations of the system trajectory between regions are proposed in a fourth part. Finally the methodology is applied to the start-up of an anaerobic plant through the realistic model ADM1.

2 Model definition and analysis

2.1 Model presentation

Since the chemostat model of Monod (15) and the first macroscopic description of the fermentation process (16) modelling of AD has been an active research topic. The first models (17, 18) were

mainly focused on the methanogenesis, considering it as the limiting step. Later the representation of the process was enriched with additional steps (acidogenesis, acetogenesis,...). Sinechal *et al.* (19) were among the first to include a step for the solubilisation of particulate substrates. Other authors focused on the inhibition by substrates other than volatile fatty acids (VFA), like nitrate (20), hydrogen (21) or even sulfated compounds (22). With time models grew in complexity, including intermediate bacterial groups and substrates. Eventually a task group of international experts in AD proposed a generic model (32 equations[2] and more than 80 parameters) called ADM1 for AD Model n°1 (see Batstone *et al.* (23)). Over the years the IWA ADM1 has evolved with add-ons (24, 25), offering an advanced description of the process dynamics. Detailed models like the ADM1 are useful to simulate an anaerobic plant (26–28), or to test numerically prior to their experimental validation monitoring and control strategies based on much simpler models. However such a thorough level of description gives highly nonlinear models which can hardly be mathematically analysed, limiting their use for the development of analytical control strategies (29).

To enable a thorough mathematical analysis we use the macroscopic representation of an AD process based on two central biological reactions proposed by Bernard *et al.* (30). This model assumes that, in a first acidogenesis step, the dissolved organic substrate, of concentration s_1, is degraded by acidogenic bacteria (x_1) into volatile fatty acids (VFA, denoted s_2) and CO_2. The growth rate of these bacteria is $\mu_1(s_1)$:

$$k_1\, s_1 \xrightarrow{\mu_1(s_1)x_1} x_1 + k_2\, s_2 + k_5\, \mathrm{CO_2}$$

In a second step (methanogenesis), the VFA are degraded into CH_4 and CO_2 by methanogenic bacteria (x_2) with growth rate $\mu_2(s_2)$:

$$k_3\, s_2 \xrightarrow{\mu_2(s_2)x_2} x_2 + k_4\, \mathrm{CH_4} + k_6\, \mathrm{CO_2}$$

The concentrations are considered to be perfectly homogeneous in the reactor, the dilution rate for the dissolved components is D and αD for the solid phase (*i.e.* the biomasses have a retention time $1/(\alpha D)$). The dynamical mass-balance model in a continuous stirred tank reactor is then straightforwardly derived (30, 31):

$$\left\{\begin{array}{lcl} \dot{s}_1 &=& D(s_{1,in} - s_1) - k_1\mu_1(s_1)x_1 \\ \dot{x}_1 &=& -\alpha D x_1 + \mu_1(s_1)x_1 \\ \dot{s}_2 &=& D(s_{2,in} - s_2) - k_3\mu_2(s_2)x_2 + k_2\mu_1(s_1)x_1 \\ \dot{x}_2 &=& -\alpha D x_2 + \mu_2(s_2)x_2 \\ q_m &=& k_4\mu_2(s_2)x_2 \end{array}\right. \tag{1}$$

$s_{1,in}$ and $s_{2,in}$ are respectively the concentration of the influent organic substrate and influent VFA, q_m the methane flow rate, and '$k_i s$' are pseudo-stoichiometric coefficients.

A Monod kinetics is chosen for the substrate-saturated growth rate of acidogenic bacteria:

$$\mu_1(s_1) \;=\; \bar{\mu}_1 \frac{s_1}{s_1 + k_{s1}} \tag{2}$$

$$\tag{3}$$

where $\bar{\mu}_1$ is the maximal growth rate of the acidogenic bacteria and k_{s1} is the half-saturation constant associated to s_1.

[2]26 differential equations to describe the behaviour of organic and inorganic matter and 6 additional equations for the acid-base reactions

The methanogenesis kinetics is represented by an Haldane equation to incorporate possible inhibition by an accumulation of VFA:

$$\mu_2(s_2) \quad = \quad \bar{\mu}_2 \frac{s_2}{s_2 + k_{s2} + \frac{s_2^2}{k_{i2}}} \tag{4}$$

where $\bar{\mu}_2$ is the potential maximum growth rate of the methanogenic bacteria, k_{s2} the potential half-saturation constant, and k_{i2} the inhibition constant.

2.2 Model reduction

First let us remark that in system (1) the acidogenic phase $(s_1;\, x_1)$ is independent of the methanogenic one $(s_2;\, x_2;\, q_m)$ and can be studied separately. Hess and Bernard (11) showed that the acidogenic phase admits a unique globally asymptotically stable equilibrium in the interior domain, meaning that the sub-system $(s_1;\, x_1)$ eventually reaches this steady-state, and that after a transient time the concentration s_1 can be considered constant. The analysis of system (1) can then be limited to the study of the methanogenesis $(s_2;\, x_2;\, q_m)$ as a stand-alone process independent of the acidogenic phase:

$$\left\{ \begin{array}{lcl} \dot{s_2} & = & D\,(\tilde{s}_{2,in} - s_2) - k_3\,\mu_2(s_2)\,x_2 \\ \dot{x}_2 & = & \mu_2(s_2)\,x_2 - \alpha\,D\,x_2 \\ q_m & = & k_4\,\mu_2(s_2)\,x_2 \end{array} \right. \tag{5}$$

where $\tilde{s}_{2,in} = s_{2,in} + \frac{k_2}{k_1} s_{1,in}$ is an upper bound for the total concentration of VFA in the digester[3].

The study of the equilibria of system (5) and the analysis of their stability give hints on the process behaviour, and we address this question in the next section.

2.3 Model analysis

2.3.1 Equilibrium and stability

In the case where solid and liquid retention times are equal ($\alpha = 1$), system (5) has been widely studied (17, 18). This is more complex for $\alpha < 1$.
For the rest of the study D and $\tilde{s}_{2,in}$ are assumed to be piecewise constant. In these conditions it has been demonstrated (11) that model (5) stays positive and that the state variables $\xi_2(t) = (s_2;\, x_2)$ remain in a bounded domain called $\mathcal{K}$.

Depending on the parameters of the model and of the operating conditions, several cases are possible for the equilibria (11) of system (5). The equilibria are solutions of the following system:

$$\left\{ \begin{array}{lcl} \dot{s}_2 & = & 0 \quad = \quad D\,(\tilde{s}_{2,in} - s_2) - k_3\,\mu_2(s_2)\,x_2 \\ \dot{x}_2 & = & 0 \quad = \quad \mu_2(s_2)\,x_2 - \alpha\,D\,x_2 \end{array} \right. \tag{6}$$

One case of special interest is when the system is bistable; in this case there are three equilibria. The trivial solution $\xi_2^\dagger$ which corresponds to the acidification of the digester is called the acidification steady-state (or acidification point). This equilibrium, characterised by a null bacterial biomass and

[3]the total concentration of VFA available for the methanogenesis is equal to the influent VFA $s_{2,in}$ plus the ones produced by the acidogenic bacteria $\frac{k_2}{D}\mu_1(s_1)$, and it can be shown that $s_{2,in} + \frac{k_2}{D}\mu_1(s_1) \leq s_{2,in} + \frac{k_2}{k_1} s_{1,in} = \tilde{s}_{2,in}$

therefore no biogas production, is given by $\xi_2^\dagger = (\tilde{s}_{2,in}, 0)$. The two interior steady-states $\xi_2^{i\star}$, for which the biomass is positive, verify:

$$\left\{ \begin{array}{lcl} \mu_2(s_2^{i\star}) & = & \alpha D \\ x_2^{i\star} & = & \frac{\tilde{s}_{2,in} - s_2^{i\star}}{\alpha k_3} \end{array} \right. \tag{7}$$

Among the two solutions, $\xi_2^{1\star}$ denotes the equilibrium with the highest biomass. In the sequel we call "working point" this equilibrium.
The study of the Jacobian matrix of system (5) for the three steady-states shows that $\xi_2^{1\star}$ and $\xi_2^\dagger$ are locally stable and $\xi_2^{2\star}$ is unstable (11, 12).

2.3.2 Attraction basin and risk index

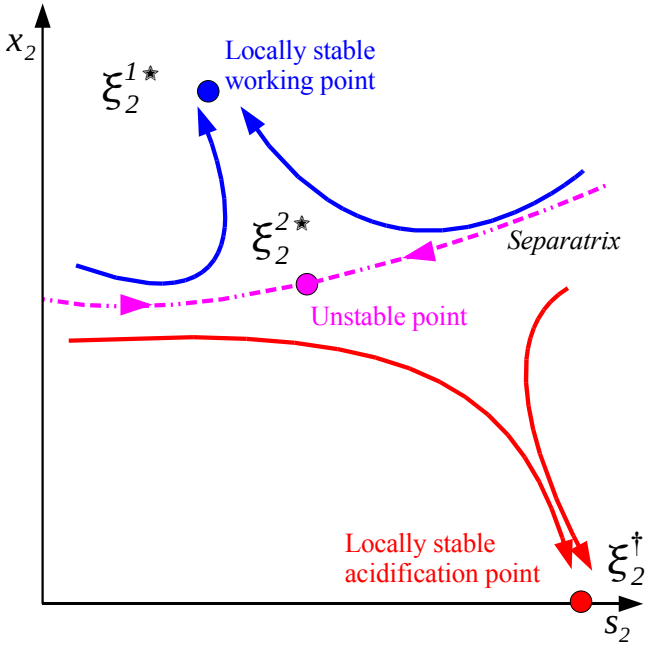

Figure 1: Possible trajectories in the phase plane: case when two steady-states are stable.

Assuming constant operating conditions, the system behaviour strongly depends on the initial conditions as illustrated on Figure 1. Indeed, for some conditions the trajectories will converge towards $\xi_2^{1\star}$ while for other they will reach $\xi_2^\dagger$. In order to evaluate the system global stability we characterise the set of initials conditions leading eventually to $\xi_2^{1\star}$.

Definition We define the **basin of attraction** of the working point as the set of initial conditions in $\mathcal{K}$ for which the process converges asymptotically towards the working point $\xi_2^{1\star}$. More formally, it is defined as:

$$\Lambda^{1\star} = \left\{ \xi_{2,0} \in \mathcal{K} \,|\, \lim_{t \to +\infty} \xi_2(\xi_{2,0}, t) = \xi_2^{1\star} \right\},$$

We define in the same way the basin of attraction $\Lambda^\dagger$ for $\xi_2^\dagger$, as the set of initial conditions leading to the process acidification:

$$\Lambda^\dagger = \left\{ \xi_{2,0} \in \mathcal{K} \,|\, \lim_{t \to +\infty} \xi_2(\xi_{2,0}, t) = \xi_2^\dagger \right\}$$

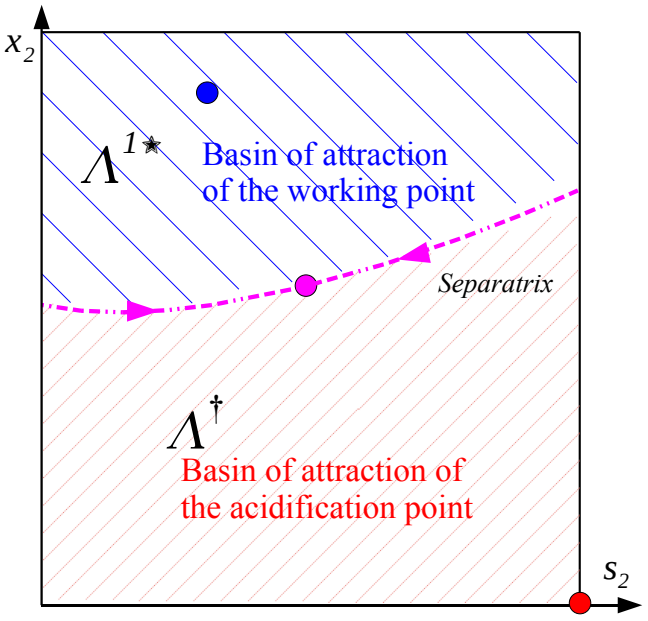

Figure 2: Attractions basins of the two locally stable equilibria.

Definition The separatrix (see Figures 1 and 2) is defined as the curve dividing the plane into the two attraction basins (it is indeed the stable manifold associated to the unstable steady-state $\xi_2^{2\star}$).

Remark: The separatrix can be computed numerically by integrating system (5) in inverse time started close to the unstable equilibrium along its stable direction.

It is worth remarking that the bigger the attraction basin $\Lambda^{1\star}$ the fewer chances that after perturbations the new initial conditions lie in $\Lambda^{\dagger}$, and that eventually the system evolves towards the acidification. This leads (11) to propose a Stability Index ($\mathcal{I}_{\mathcal{S}}$) based on the relative size of the attraction basin of the working point:

$$\mathcal{I}_{\mathcal{S}} = \frac{\mathcal{S}(\Lambda^{1\star})}{\mathcal{S}(\mathcal{K})}$$

where $\mathcal{S}$ is the area of the considered domain .

Ideally the plant manager should choose operating conditions that maximise $\Lambda^{1\star}$ in order to limit the risk of destabilisation. Yet in practice the operator has to simultaneously process a maximal loading and prevent a plant failure.

The weakness of this index of stability $\mathcal{I}_{\mathcal{S}}$ is that it does not depend on the real state of the process. As shown on Figure 3 the operating conditions may guarantee a large attraction basin for the useful working point (low risk), but with inappropriate initial conditions the system would however converge towards the acidification point. Moreover, as illustrated on Figure 4 for trajectories close to the separatrix, which were *a priori* in the working attraction basin, small perturbations (here a slight hydraulic overload) can make the system diverge leading to the failure of the plant.

In order to propose a monitoring procedure more strongly related to the actual process state, we study the transient behaviour of the system and finally evaluate on which side of the separatrix the system evolves.

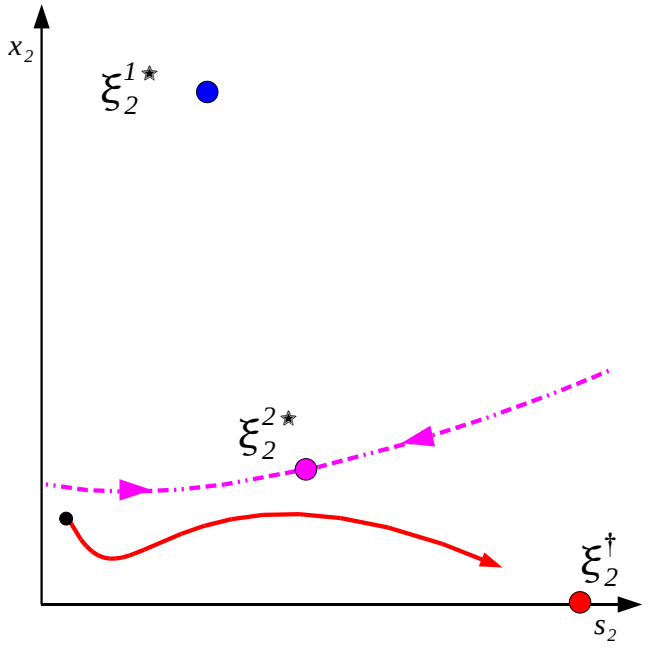

Figure 3: Case of low risk index but with a trajectory initiated towards the acidification point.

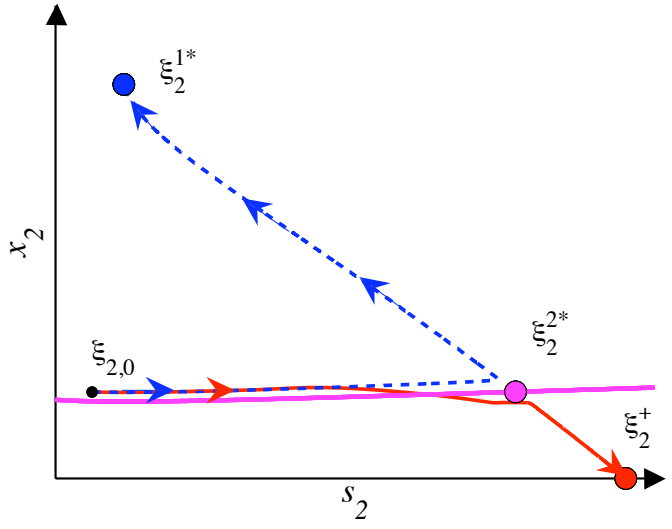

Figure 4: Simulation of possible bifurcations of the system due to a slight hydraulic overload that moves the system to the other side of the separatrix: trajectories in the phase plane (- -) without perturbations, (–) with perturbations.

3 Study of the phase plane

Often, in biology, the models and their parameters are not perfectly known making the accurate prediction of system's behaviour a tough task. The key idea of qualitative reasoning methods (32, 33) is to derive the qualitative dynamics of the system from the analysis of the model structure. In the case of low dimensional systems phase space analysis allow to approach the qualitative behaviour (13, 14, 34, 35) independently of parameter values. In the following section we assess the qualitative dynamical behaviour of system (5) using the approach developed in (13, 36).

3.1 Partitioning of the phase plane

Similarly to Bernard and Gouzé (13) we split the phase plane, *i.e.* the space $(s_2;\, x_2)$, into regions where the variables have a fixed trend (see Figure 5). We consider the nullclines which are the curves where the derivative of a variable cancels. Nullclines are thus computed by solving individually the following equations: $\dot{x}_2 = 0$, $\dot{s}_2 = 0$, $\dot{q}_m = 0$. When a nullclines is crossed it means that the sign of the derivative of the associated variable switches, leading thus to an extremum. We also consider the separatrix and specific thresholds $s_2 = s_2^m$ and $x_2 = x_2^m$, where s_2^m is the value that maximises the growth rate $\mu_2(s_2)$ and x_2^m the intersection of the s_2-nullcline with the line $s_2 = s_2^m$. At the end it leads to 21 regions[4] where the sign of $(\dot{x}_2,\, \dot{s}_2,\, \dot{\mu}_2,\, \dot{q}_m)$ is constant:

- The nullclines for s_2, x_2 and for q_m split the domain $\mathcal{K}$ into 9 regions.
- The lines $s_2 = s_2^m$ and $x_2 = x_2^m$ divide $\mathcal{K}$ into 4 regions.
- The separatrix splits some of these regions into two zones.

We gather some zones with similar characteristics and we consider in the sequel only 19 zones[5] (see Figure 5). The qualitative characteristics $(\dot{x}_2,\, \dot{s}_2,\, \dot{\mu}_2,\, \dot{q}_m)$ of this phase plane are summarised in Table 1. It is worth noting that the q_m-nullcline almost coincides with the s_2-nullcline in zone 1.

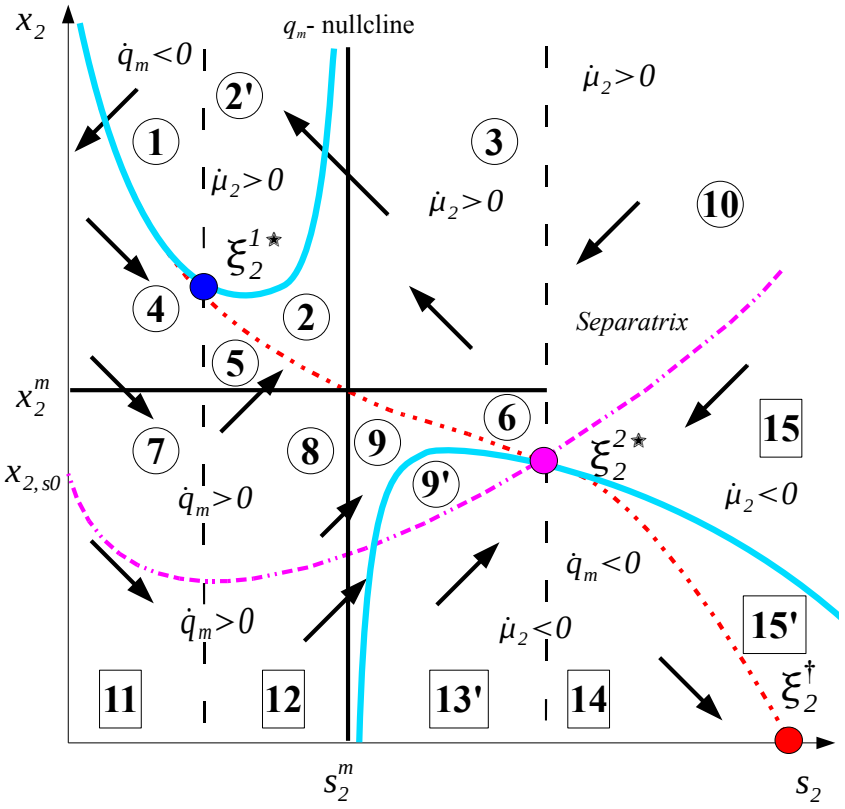

Figure 5: Phase plane with the separatrix and the nullclines for s_2 (· · —), x_2 (- -) and q_m (–).

[4] a numerical study for a wide range of operating conditions ($D \in [.1; 1.05]$ d^{-1} and $s_{2,in} \in [3; 200]$ mmol.L^{-1}) of the relative position of x_2^m with respect to the intersection $x_{2,s0}$ of the separatrix and the axis $s_2 = 0$ shows that the inequality $x_2^m > x_{2,s0}$ always holds.

[5] indeed zone 2, 9, 13 and 15 are divided in two by the q_m-nullcline

Table 1: Qualitative signature of the subdivisions of the phase plane.

sign \ zone	1	2	2'	3	4	5	6	7	8	9	9'	10	11	12	13	13'	14	15	15'
$\dot{x}_2$	-	+	+	+	-	+	+	-	+	+	+	-	-	+	+	+	-	-	-
$\dot{s}_2$	-	-	-	-	+	+	-	+	+	+	+	-	+	+	+	+	+	-	-
$\dot{\mu}_2$	-	-	-	+	+	+	+	+	+	-	-	+	+	+	-	-	-	+	+
$\dot{q}_m$	-	-	+	+	+	+	+	+	+	+	-	+	+	+	+	-	-	+	-

With this partitioning we see that the sign of the vector $(\dot{x}_2,\ \dot{s}_2,\ \dot{\mu}_2,\ \dot{q}_m)$ at an instant is not sufficient to identify in which zone the system lies: for example it appears in Table 1 that zones 5, 8 and 12 have the same qualitative signature (+, +, +, +). Indeed only six groups of zones (1, 2, 2', 3+6, 14 and 15') have a unique signature, specific to one side of the separatrix. For the other zones, similar qualitative characteristics may correspond to zones on both side of the separatrix as shown in Table 2.

Table 2: Indistinguishable zones on the basis of the sign of vector $(\dot{x}_2,\ \dot{s}_2,\ \dot{\mu}_2,\ \dot{q}_m)$.

Zones with similar characteristics					
$\Lambda^{1\star}$	4 and 7	5 and 8	9	9'	10
$\Lambda^{\dagger}$	11	12	13	13'	15

It is clear from Tables 1 and 2 that the instantaneous trends do not provide a precise positioning of the trajectory at time t, and it is essential to derive methods to assess on which side of the separatrix the system is. For this we study the successive transitions between these regions and show that they can clear up the ambiguities.

3.2 Characterisation of the trajectories with transition graphs

We consider the complete phase plane of Figure 5 and we determine, according to the vectors field $(\dot{s}_2,\ \dot{x}_2)$, the possible transitions of the trajectories[6] from one zone to another. For example according to the vector field, the trajectory of the system has to cross the q_m-nullcline to go from zone 2 (where q_m is increasing) to zone 2' (where q_m is decreasing) (see Table 1). Thus this transition corresponds to a maximum of the biogas flow-rate.

We use the following symbolism to represent the transitions of the trajectories:

- M is a transition through a maximum (M_x represents a maximum of the biomass x_2 and M_s a maximum of the VFA s_2),
- m is a transition through a minimum (m_x represents a minimum of the biomass x_2 and m_s a minimum of the VFA s_2),
- T is an increasing transition through the lines $x_2 = x_2^m$ or $s_2 = s_2^m$,
- t is an decreasing transition through the lines $x_2 = x_2^m$ or $s_2 = s_2^m$.

[6] we neglect the zero dimensional set of trajectories that cross 2 zones at the same time.

This leads to the transition graphs (13) represented on Figure 6.

Since the trajectories are bounded, it is worth remarking that they cannot stay trapped in a zone, unless they reach a steady-state (36). This is possible only from the zones where the state variables are increasing under their equilibrium value or decreasing above. Thus, only zones 2 and 4 in $\Lambda^{1\star}$ and 14 in $\Lambda^{\dagger}$ can be the final zones leading to the steady-state.

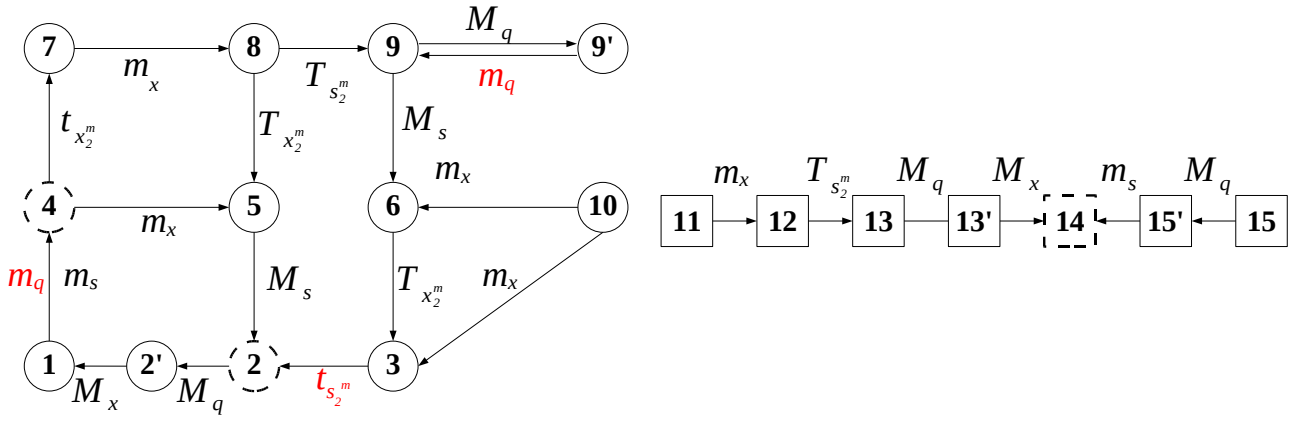

Figure 6: Possible dynamical trajectories and transitions of the system in $\Lambda^{1\star}$ (left figure), $\Lambda^{\dagger}$ (right figure).

It is worth noting that some transitions are specific to the working attraction basin $\Lambda^{1\star}$ and their occurrence guaranties that the system is on the right side of the separatrix:

- A minimum of the biogas flow rate (m_q) can only be observed from zone 1 to zone 4 and from zone 9' to zone 9.
- A transition through a maximum of the substrate M_s only occurs from zone 9 to zone 6 and from zone 5 to zone 2.
- The decreasing transition through $s_2 = s_2^m$ is specific to a trajectory from zone 3 to zone 2.

3.3 Design of a risk index

The transition graph for $\Lambda^{\dagger}$ clearly shows that after a transient time the system enters zone 14 which is a dead-end. Once system (5) enters this part of the plane it can only converge towards the acidification equilibrium. On the contrary there exist possible cycles and no clear terminal zone for $\Lambda^{1\star}$: the convergence towards the useful equilibrium $\xi_2^{1\star}$ appears less straightforward and even with favourable initial conditions, the system can pass through zones close to the separatrix before converging (see Figure 4). In such a case even small perturbations can jeopardise the system stability.

The convergence towards $\xi_2^{1\star}$ is only possible in zones 2 and 4 and so when the system is in one of these zones it is likely to reach the steady-state. These two zones can then be considered as safe. Similarly zone 1 is characterised by a high biomass and a decreasing substrate (see Figure 5 and Table 1) and as such it can be considered as one of the safest part of the plane. We then propose a risk index associated to the minimal number of zones the system has to cross (*i.e* the number of transitions) before reaching the *convergence regions* (zone 2 and 4 in $\Lambda^{1\star}$). In the same way for $\Lambda^{\dagger}$, we classify the risk by the number of transitions before the system reaches zone 14. Table 3 presents this ranking.

Table 3: Risk ranking of the phase plan (I.R.: inhibition region, C.R.: convergence region).

Risk		Ranking	Nb of transitions	Zone	Comment
		1	0	2	C.R.
		2	1	1	
		3	1	5	
		4	0	4	C.R.
		5	2	3	I.R.
		6	2	2'	
	in $\Lambda^{1\star}$	7	2	8	
		8	2	6	I.R.
		9	3	7	
		10	3	9	I.R.
		11	3	10	I.R.
		12	4	9'	I.R.
		13	4	11	
		14	3	12	
		15	3	13	I.R.
	in $\Lambda^{\dagger}$	16	1	13'	I.R.
		17	2	15	I.R.
		18	1	15'	I.R.
		19	0	14	I.R., C.R.

3.4 Dynamical monitoring of the system

In this section we show that the monitoring of the successive transitions allows to identify the system position in the phase plane.

In order to illustrate this approach we consider on Figure 7 two possible trajectories initialised on both sides of the separatrix; the first sequence characterises a trajectory in $\Lambda^{1\star}$ initialised in region 7 and the second one a trajectory in $\Lambda^{\dagger}$ initialised in zone 11. The corresponding transitions sequences extracted from the transition graphs of Figure 6 are represented on Figure 7.

For these two examples we see that the first three transitions ($m_x \rightarrow T_s \rightarrow M_q$) are the same for both trajectories, while the fourth transition (m_q *vs.* M_x) discriminates the two trajectories, and this way locates the position of the system in the phase plane.

It is then clear that if we monitor the trends, *i.e.* the sign of $(\dot{x}_2,\ \dot{s}_2,\ \dot{\mu}_2,\ \dot{q}_m)$ on a sufficiently long period we can not only identify the region of the space where the system is and identify the associated risk, but we can also assess the trajectory history. For example we see on Figure 8 that close initial conditions can lead to opposite final state. The associated successive extrema and transitions can be seen on Figure 8 and the fourth transitions (m_q in $\Lambda^{1\star}$ or M_x in $\Lambda^{\dagger}$) which are decisive to discriminate the two trajectories can be detected before the system reaches its steady-state.

It is worth noting that this property is generic and does not depend on the parameters values. With a variation in the parameters the exact position of the zones is likely to change but the qualitative transitions would remain the same. This approach can then be applied even without knowing the model parameters.

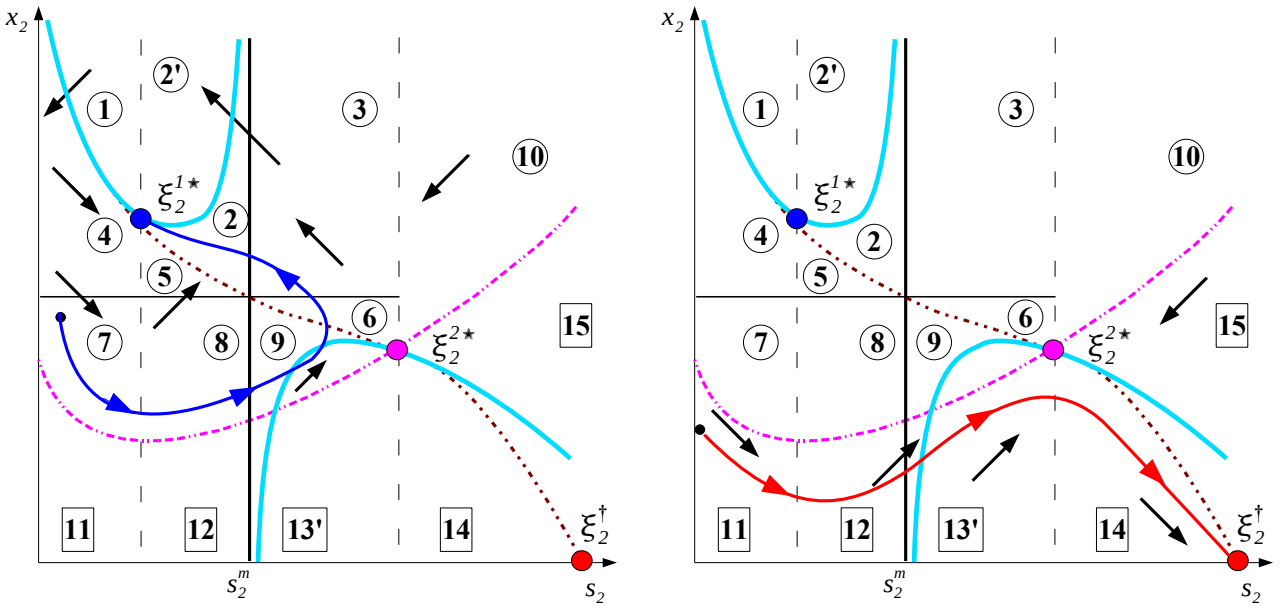

Figure 7: Trajectories and associated sequence of transitions in $\Lambda^{1\star}$ (left), in $\Lambda^{\dagger}$ (right).

3.5 Qualitative monitoring with partial available information

So far the analysis was done assuming that all the variables were measured (even qualitatively) which is not realistic. In practise only the VFA and the methane flow rate may be easily measured. If only the trends of s_2 and q_m are detected, we can derive sub-graphs from the transition graphs of Figure 6 keeping only the transitions for s_2 and q_m.

The transitions $T_{s_2^{2\star}}$, $t_{s_2^{2\star}}$ and $t_{s_2^{1\star}}$ need the values $s_2^{1\star}$ and $s_2^{2\star}$ to be detected. They depend on the parameters of the model which can hardly be perfectly known. It is however possible to bound these values considering upper and lower limits for the parameters. These additional transitions are useful since they can easily discriminate trajectories on both sides of the separatrix. The obtained sub-graphs are represented on Figure 9.

These graphs show that any **sequence of three transitions** is decisive to qualitatively identify the state of the system. Indeed a sequence of two transitions is not sufficient as the sequence $T_{s_2^m} \to M_q$ is possible in the two basins (zone 8 to zone 9 in $\Lambda^{1\star}$ or zone 12 to zone 13 in $\Lambda^{\dagger}$). It is a problem because in $\Lambda^{\dagger}$ these transitions eventually lead to the acidification steady-state. However it is worth remarking that this sequence corresponds to a low biomass and a relatively high VFA concentration. As such it is a situation that the operator should detect easily (*e.g.* with a low biogas flow rate).

In the next section we apply the method for monitoring the start-up of an AD plant.

4 Application: monitoring the start-up of an AD plant

4.1 Objectives

AD is known to be very delicate to manage especially during the process start-up which might be considered as the most unstable phase in AD (37). The key difficulty is to achieve a trade-off between rapid start-up and process stability. It means that the organic loading rate must be increased as fast as

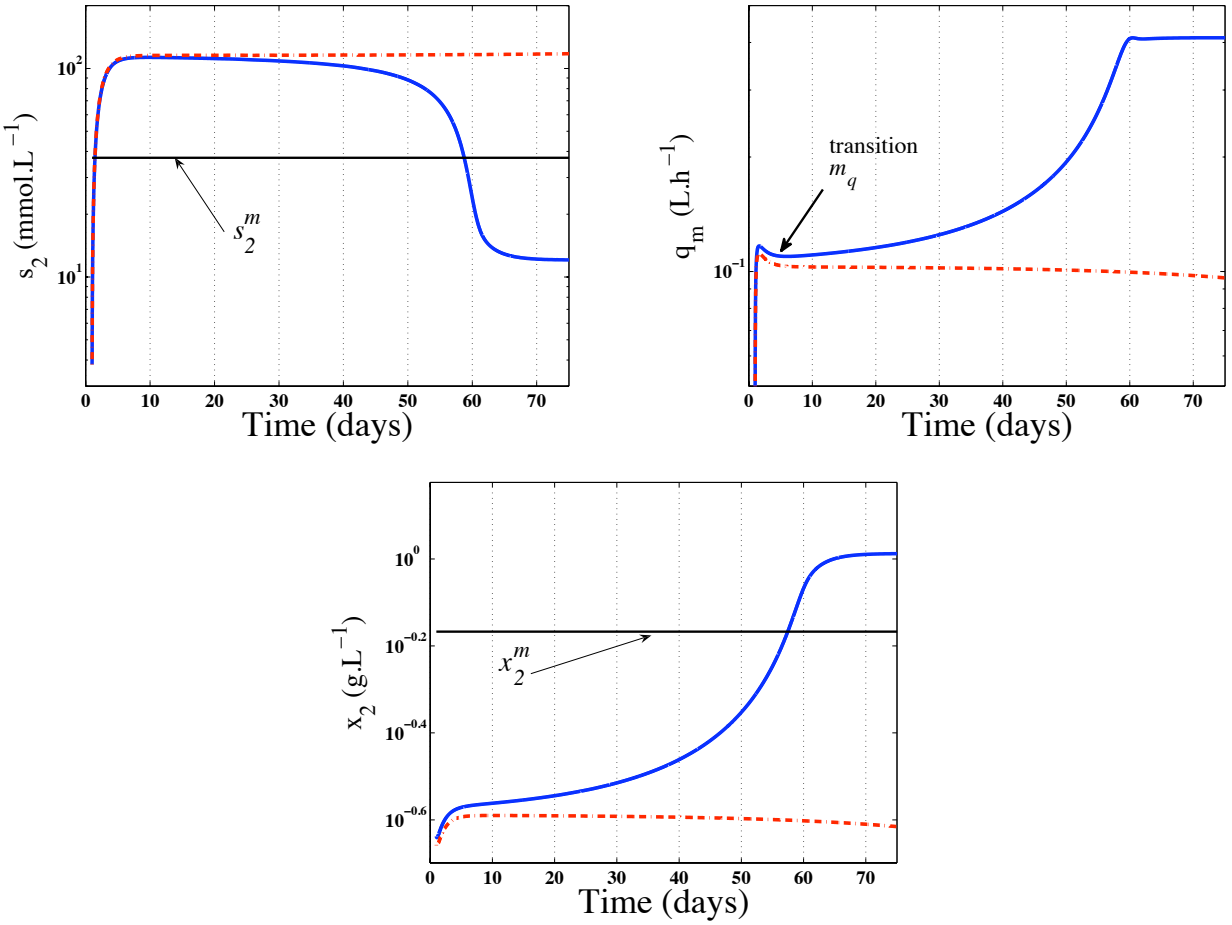

Figure 8: Simulation of the trajectories as presented on Figure 7 with close initial conditions on both sides of the separatrix: (–) in $\Lambda^{1\star}$, (·—) in $\Lambda^{\dagger}$.

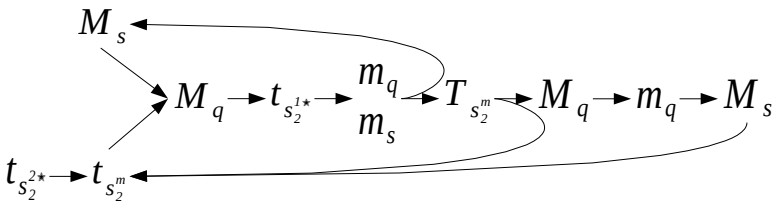

$$\begin{cases} T_{s_2^m} \rightarrow M_q \rightarrow T_{s_2^{2\star}} \\ \dot{s}_2 > 0 \end{cases} \qquad \begin{cases} M_q \rightarrow m_s \\ s_2 > s_2^{2\star} \end{cases}$$

Figure 9: Transitions sequences in $\Lambda^{1\star}$ (upper graph) and $\Lambda^{\dagger}$ (lower graph) with partial knowledge of the state.

possible, avoiding at the same time the acidification of the reactor. However due to the slow growth rate of methanogenic bacteria, disturbances such as an overload or an inhibitor may lead to the process

failure (38). Reactor start-up is then a long procedure (from 1 month to almost one year) which is essential to achieve a high treatment capacity at steady-state (39), and therefore this phase should be operated meticulously. To this end many studies aimed at identifying key-parameters influencing the methanogenic biomass development as the hydraulic retention time (40) or the nutrients (38, 41). On this basis several authors have developed monitoring strategies to adapt the OLR to the biomass treatment capacity, assessed for example on the basis of the specific methanogenic activity (42) or the methane yield (43) or other proxies, thus limiting the risk of reactor acidification. In this section we illustrate a possible use of our monitoring strategy by including it in a rule-based protocol to achieve a fast digester start-up.

4.2 Start-up algorithm

Considering the transition graph of Figure 9 we propose a simple algorithm to progressively increase the feed flow rate and monitor the response of the plant to this increase. It is based on the qualitative features of methane and VFA during a period of time, and a decision is taken at the end of each period based on the following rules:

Case 1. If there is a transition through a minimum of the biogas flow rate (m_q) or through a maximum of the VFA concentration (M_s), it means that the system evolves towards the useful working point. Hence the feed flow rate can be increased.

Case 2. If no transition m_q or M_s is detected, it is considered that the bacteria are not yet acclimated to the OLR and they should be given more time. So the influent feed flow is kept at the same value for one more period of time.

Case 3. If after two attempts (*i.e.* two periods with identical operating conditions) no discriminating transition (m_q or M_s) has occurred, the OLR is considered to be beyond the maximum treatment capacity of the bacterial population and the influent feed flow Q_{in} is decreased.

Case 4. If Q_{in} had to be decreased more than 4 times, the system is suspected of evolving towards the acidification and the start-up procedure is stopped. In this case the algorithm parameters must be tailored, for example by reducing the height of the step changes, or increasing the duration after each changes to give more time to the system to adapt to the new operating conditions.

Besides to limit the risk of acidification after each step change of the feed flow rate, the closer to the maximal OLR the smaller the amplitude of the steps, and the longer the time given to the system before analysing the signals q_m or s_2.

4.3 Application using the ADM1 model

Model ADM1 was used to simulate an anaerobic fixed-bed start-up. The model was calibrated with data obtained during the start-up of a fixed-bed reactor at the LBE-INRA in Narbonne, France (see Steyer *et al.* (44) for more details on the process). The parameters used are the ones given for mesophilic high-rate digesters in the technical report on ADM1 (23), with a tuning of the Monod specific growth rate of the acetate degrading bacteria, the half-saturation constant for the hydrogen degradation and the retention time of the solids (see Table 4).

We assume that the influent concentration is 35 gCOD.L^{-1} (with 20% of the COD due to the VFA see Table 5). The increase of the OLR must start from 0.5g COD.L^{-1}.d^{-1} to reach 35 gCOD.L^{-1}.d^{-1} at the end through the increase of the feed flow rate (Q_{in}). The reactor temperature and the pH are

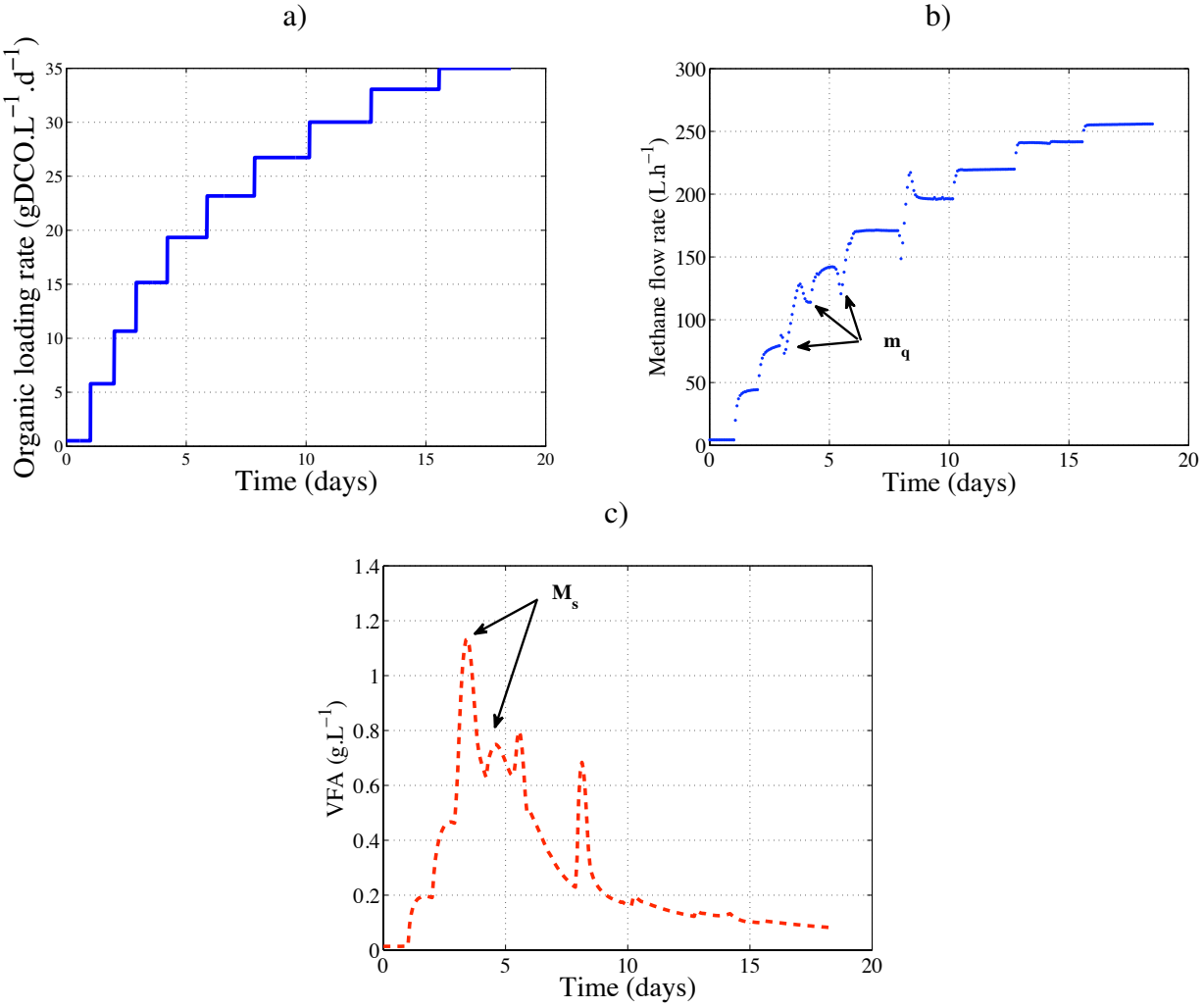

Figure 10: Application of the monitoring strategy to the start-up of a digester: a) Organic loading rate, b) Biogas flow-rate, c) Volatile fatty acids.

Table 4: Modified parameters used for the simulations of ADM1 with respect to the values in Batstone *et al.* (23)

Monod specific uptake rate for acetate degrading bacteria (k_{m_ac})	13.5 COD·COD^{-1}·d^{-1}
Half-saturation constant for hydrogen degradation ($K_{s\_h_2}$)	2.5·10^{-5} kg COD·m^{-3}
Retention time of the solids ($t_{res,X}$)	100 d

supposed to be respectively regulated at 35°C and 6.9. Figure 10 shows that the start-up is achieved in less than 20 days.

Table 5: Influent composition for the simulations of ADM1

Total influent concentration	35 gCOD.L^{-1}
Carbohydrates	80.19%
Acetate	13.21%
Propionate	6.6%
Butyrate	0%
Valerate	0 %

Once the desired OLR is reached the digester is operated continuously with the final OLR conditions. This strategy is compared on Figure 11 with a classical exponential increase of the OLR where the feed flow rate is increased on a daily basis. The exponential increase leads the reactor to the acidification up to 14.5 $g.L^{-1}$ of VFA, while, for the rule-based algorithm, the VFA never exceed 1.13 $g.L^{-1}$. Figure 11 shows that the methane production in the exponential increase, rapidly reaches a value close to zero, while with the start-up protocol it keeps increasing until it reaches a maximum value of 255 $L.h^{-1}$.

In the application of the proposed algorithm, case 1 is the most frequently met (minimum of biogas can be seen *e.g.* at time t=3, 4, or 5.5 days on Figure 10 b), and a maximum of the VFA concentration M_s is detected at time t=3.5 or 5.5 days (Figure 10 c). Finally the organic flow rate was never decreased to reach the requested OLR safely.

It is worth noting that the rule-based algorithm does not impose a minimum COD removal efficiency before increasing the OLR. It ensures that the feed flow rate is increased only when the system is able to cope with a higher OLR even though the VFA concentration is high. This allows to reduce the time between each change of the OLR which quicken the start-up. Surprisingly, the COD removal is always higher than 90% (graphs not shown). Another interesting feature of the proposed protocol is that the OLR is always higher than with the exponential strategy. This approach is close to the empirical approaches proposed by Steyer *et al.* (7) and Liu *et al.* (8) who analyse qualitatively the response of the process after each step change of the organic loading rate to decide whether to increase or decrease the OLR.

5 Conclusion

In this paper we have studied the dynamical behaviour of a simple model of AD. We have shown how qualitative events such as extrema or crossing of some values can be used to identify in which part of the space the trajectory lies. This approach can be deployed even on the basis of partial knowledge, *i.e.* in the most standard case where biomass is not measured. The monitoring of the trends of some variables, for example the sign of $(\dot{s}_2,\ \dot{q}_m)$, allows to assess an associated dynamical risk. Thereby this methodology completes the static criterion proposed in Hess and Bernard (11) that demonstrated its efficiency on real data.

On this basis a methodology using the monitoring of the extrema of the VFA and the methane flow rate was applied to control the increase of the organic loading rate during a start-up phase. Simulations with model ADM1 showed that a fast and secure start-up (less than 20 days) could be achieved with a simple rule-based algorithm controlling the dilution rate. The proposed strategy proved itself to be more efficient than a classical exponential increase of the OLR which led the process to failure. Our approach could also be used for other purposes than process start-up. For example it can help to detect a perturbation and help the system to go back to normal, or at any time it can be used to diagnose the process state.

The presented properties rely on a simple model which captures the essential dynamics and stability rules of AD process. The proposed method does not depend on the parameter values, which makes it rather generic and widely applicable: this approach based on qualitative properties can be applied even without knowing the model parameters and is thus very robust.

The next step would consist in using state observers to estimate the unmeasured variables, as the biomass, or the biomass growth rate (45, 46). With this additional information it would be possible to use the detailed transition graphs rather than the partial ones, in order to end-up with a more accurate process monitoring.

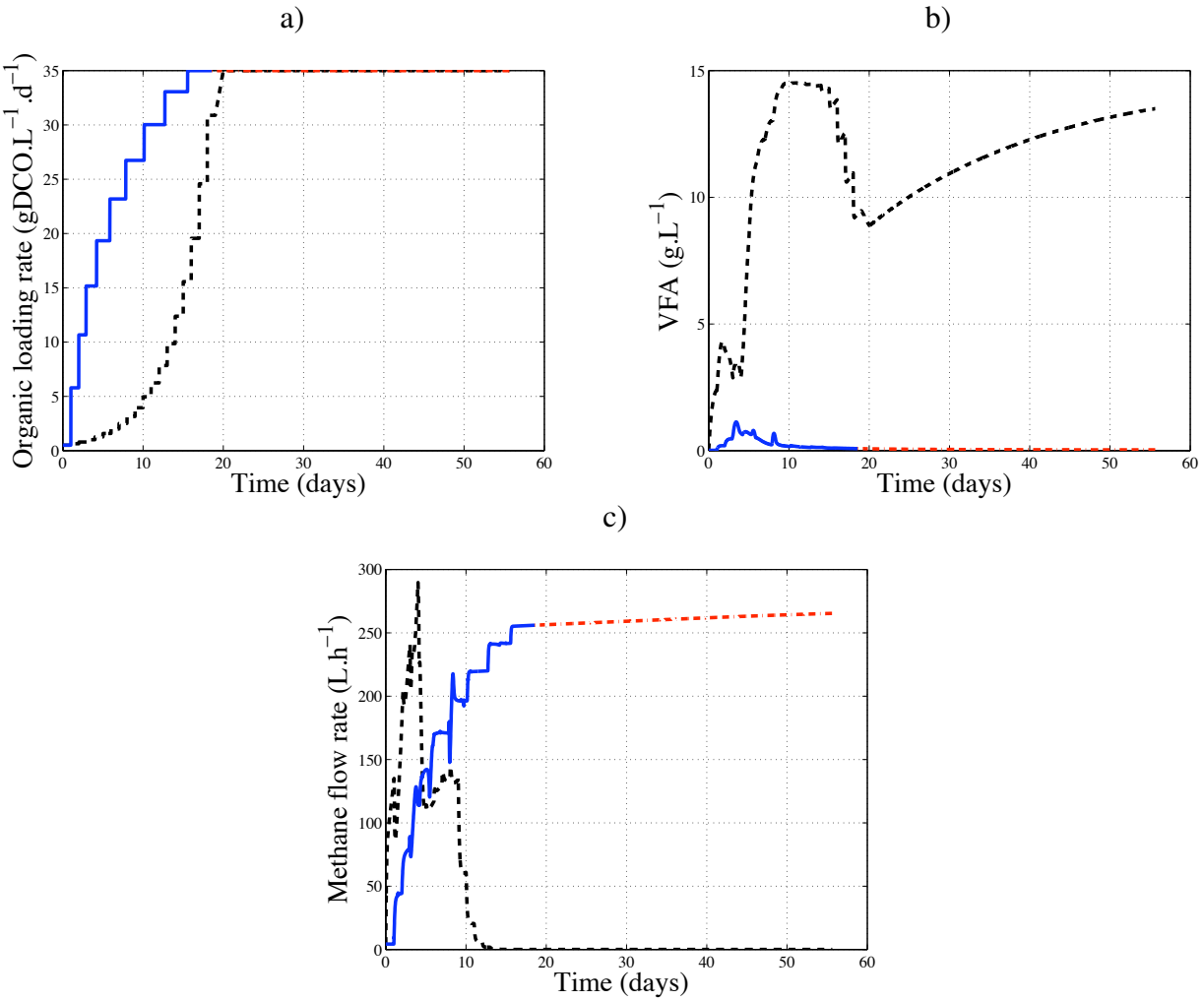

Figure 11: Comparison of the monitored start-up with a linear increase strategy: (- -) exponential increase, (–) rule-based increase, (·—) steady-state run

Acknowledgement

J.Hess thesis was funded both by ADEME and by the Provence-Alpes-Cotes-d'Azur Region. This work benefited from the support of the INRIA for the CODA ARC.

Nomenclature

AD	Anaerobic Digestion
OLR	Organic Loading Rate
VFA	Volatile Fatty Acids

D	dilution rate	d^{-1}
k_1	yield for substrate degradation	
k_2	yield for VFA production	$\mathrm{mmol.g}^{-1}$
k_3	yield for VFA degradation	$\mathrm{mmol.g}^{-1}$
k_4	yield for methane production	$\mathrm{mmol.g}^{-1}$
k_5	yield for CO_2 production from organic substrate	$\mathrm{mmol.g}^{-1}$
k_6	yield for CO_2 production from VFA	$\mathrm{mmol.g}^{-1}$
k_{i2}	inhibition constant for the methanogenesis	$\mathrm{mmol.L}^{-1}$
k_{s1}	half-saturation constant for the acidogenesis	$\mathrm{g.L}^{-1}$
k_{s2}	half-saturation constant for the methanogenesis	$\mathrm{g.L}^{-1}$
q_m	methane flow-rate	$\mathrm{mmol.L}^{-1}\mathrm{.d}^{-1}$
s_1	organic substrate concentration	$\mathrm{g.L}^{-1}$
$s_{1,in}$	influent organic substrate concentration	$\mathrm{g.L}^{-1}$
s_2	VFA concentration	$\mathrm{mmol.L}^{-1}$
$s_{2,in}$	influent VFA concentration	$\mathrm{mmol.L}^{-1}$
$\tilde{s}_{2,in}$	upper bound for the total VFA concentration	$\mathrm{mmol.L}^{-1}$
x_1	concentration of acidogenic bacteria	$\mathrm{g.L}^{-1}$
x_2	concentration of methanogenic bacteria	$\mathrm{g.L}^{-1}$
α	fraction of free biomass in the liquid medium	
μ_1	acidogenic bacteria growth rate	d^{-1}
$\bar{\mu}_1$	maximum acidogenic growth rate	d^{-1}
μ_2	methanogenic bacteria growth rate	d^{-1}
$\bar{\mu}_2$	potential maximum methanogenic growth rate	d^{-1}
ξ	state vector of the process variables	
M_q	maximum of the biomethane flow-rate q_m	
m_q	minimum of the biomethane flow-rate q_m	
M_s	maximum of the VFA s_2	
m_s	minimum of the VFA s_2	
$T_{s_2^m}$	increasing transition through $s_2 = s_2^m$	
$t_{s_2^m}$	decreasing transition through $s_2 = s_2^m$	
$t_{s_2^{i\star}}$	decreasing transition through the equilibrium $s_2 = s_2^{i\star}$	
M_x	maximum of the methanogenic biomass x_2	
m_x	minimum of the methanogenic biomass x_2	
$T_{x_2^m}$	increasing transition through $x_2 = x_2^m$	
$t_{x_2^m}$	decreasing transition through $x_2 = x_2^m$	
$T_{s_2^{2\star}}$	increasing transition through the equilibrium $s_2 = s_2^{2\star}$	

References

1. Angelidaki, I.; Ellegaard, L.; Ahring, B. K. In *Biomethanation II*; Springler, **2003**, Chapter Applications of the anaerobic digestion process, 1–33.

2. Delbès, C.; Moletta, R.; Godon, J.-J. Bacterial and archaeal 16S rDNA and 16S rRNA dynamics

during an acetate crisis in an anaerobic digestor ecosystem. *FEMS Microbiology Ecology* **2001**, *35*, 19–26.

3. Fripiat, J.; Bol, T.; R. Binot, H. N.; Nyns, E. A strategy for the evaluation of methane production from different types of substrate biomass. In *Biomethane, Production and uses*, Buvet, R., Fox, M., Picker, D., Eds.; Roger Bowskill ltd: Exeter, UK, **1984**, 95–105.

4. Steyer, J.-P.; Aceves, C.; Ramirez, I.; Elias, A.; Hess, J.; Bernard, O.; Nielsen, H. B.; Boe, K.; Angelidaki, I. Optimizing biogas production from anaerobic digestion. *Proceedings of WEFTEC.06*, Dallas, US, **2006**.

5. Renard, P.; Van Breusegem, V.; Nguyen, M.-T.; Naveau, H.; Nyns, E.-J. Implementation of an Adaptative Conroller for the Startup and Steady-State Running of a Biomethanation Process Operated in the CSTR. *Biotechnology and Bioengineering* **1991**, *38* (8), 805–812.

6. Pullammanappallil, P.; Harmon, J.; Chynoweth, D. P.; Lyberatos, G.; Svoronos, S. A. Avoiding Digester Imbalance Through Real-Time Expert System Control of Dilution Rate. *Applied Biochemistry and Biotechnology* **1991**, *28-29*, 33–42.

7. Steyer, J.-P.; Buffière, P.; Rolland, D.; Moletta, R. Advanced Control of Anaerobic Digestion Processes through Disturbances Monitoring. *Water Research* **1999**, *33* (9), 2059–2068.

8. Liu, J.; Olsson, G.; Mattiasson, B. Monitoring and Control of An Anaerobic Upflow Fixed-Bed Reactor for High-Loading-Rate Operation and Rejection of Disturbances. *Biotechnology and Bioengineering* **2004**, *87* (1), 44–55.

9. von Sachs, J.; Meyer, U.; Rys, P.; Feitkenhuer, H. New approach to control the methanogenic reactor of a two-phase anaerobic digestion system. *Water Research* **2003**, *37* (5), 973–982.

10. Åkesson, M.; Hagander, P.; Axelsson, J.-P. A probing feeding strategy for *Escherichia coli* cultures. *Biotechnology Techniques* **1999**, *13*, 523–528.

11. Hess, J.; Bernard, O. Design and study of a risk management criterion for an unstable anaerobic wastewater treatment process. *Journal of Process Control* **2008**, *18* (1), 71–79.

12. Shen, S.; Premier, G. C.; Guwy, A.; Dinsdale, R. Bifurcation and stability analysis of an anaerobic digestion model. *Nonlinear Dynamics* **2007**, *48*, 391–408.

13. Bernard, O.; Gouzé, J.-L. Global qualitative behavior of a class of nonlinear biological systems: application to the qualitative validation of phytoplankton growth models. *Artificial Intelligence* **2002**, *136* (1), 29–59.

14. de Jong, H. Qualitative simulation and related approaches for the analysis of dynamic systems. *Knowledge Engineering Review* **2004**, *19* (2), 93–132.

15. Monod, J. *Recherches sur la croissance des cultures bactériennes*; Hermann & cie, 1942.

16. Illinois State Water Survey Division, *Anaerobic Fermentations*; State of Illinois, 1939.

17. Andrews, J. F. A Mathematical Model for the Continous Culture of Microorganisms Utilizing Inhibitory Substrates. *Biotechnology and Bioengineering* **1968**, *10*, 707–723.

18. Graef, S. P.; Andrews, J. F. Mathematical modeling and control of anaerobic digestion. *Water*, **1973**.

19. Sinechal, X. J.; Installe, M. J.; Nyns, E.-J. Differentiation between acetate and higher volatile acids in the modeling of the anaerobic biomethanation process. *Botechnology Letters* **1979**, *1* (8), 309–314.

20. Hill, D. T.; Barth, C. L. A dynamic model for simulation of animal waste digestion. *Journal WPCF* **1977**, *10*, 2129–2143.

21. Mosey, F. E. Mathematical modelling of the anaerobic digestion process : regulatory mechanisms for the formation of short-chain volatile acids from glucose. *Water Science and Technology* **1983**, *15*, 209–232.

22. Kalyuzhnyi, S.; Sklyar, V.; Kucherenko, I.; a Russkova, J.; Degtyaryova, N. Methanogenic biodegradation of aromatic amines. *Water Science and Technology* **2000**, *42* (5-6), 363–370.

23. Batstone, D. J.; Keller, J.; Angelidaki, I.; Kalyuzhnyi, S. V.; Pavlostathis, S. G.; Rozzi, A.; Sanders, W. T. M.; Siegrist, H.; Vavilin, V. A. *Anaerobic Digestion Model No. 1 (ADM1)*; IWA Publishing, 2002; Vol. 13.

24. Batstone, D. J.; Keller, J.; Steyer, J.-P. A review of ADM1 extensions, applications, and analysis: 2002-2005. *Water Science and Technology* **2006**, *54* (4), 1–10.

25. Fedorovich, V.; Lens, P.; Kalyuzhnyi, S. Extension of Anaerobic Digestion Model No. 1 with processes of sulfate reduction. *Applied Biochemistry and Biotechnology* **2007**, *109* (1-3), 33–45.

26. Batstone, D. J.; J.Keller, Industrial applications of the IWA anaerobic digestion model No. 1. *Water Science and Technology* **2003**, *47* (12), 199–206.

27. Parker, W. J. Application of the ADM1 model to advanced anaerobic digestion. *Bioresource Technology* **2005**, *96*, 1832–1842.

28. Rosen, C.; Vrecko, D.; Gernaey, K. V.; Pons, M. N.; Jeppsson, U. Implementing ADM1 for plant-wide benchmark simulations in Matlab/Simulink. *Water Science and Technology* **2006**, *54* (4), 11–9.

29. Simeonov, I.; Stoyanov, S. Modelling and Dynamic Compensator Control of the Anaerobic Digestion of Organic Wastes. *Chemical & Biochemical Engineering Quaterly* **2003**, *17* (4), 285–292.

30. Bernard, O.; Hadj-Sadok, Z.; Dochain, D.; Genovesi, A.; Steyer, J.-P. Dynamical model development and parameter identification for an anaerobic wastewater treatment process. *Biotechnology and Bioengineering* **2001**, *75*, 424–438.

31. Bastin, G.; Dochain, D. *On-line estimation and adaptive control of bioreactors*; Elsevier, 1990.

32. Kuipers, B. Commonsense Reasoning about Causality: Deriving Behavior from Structure. *Artificial Intelligence* **1984**, *24*, 169–203.

33. Kuipers, B. Qualitative Simulation. *Artificial Intelligence* **1986**, *29*, 289–338.

34. Lee, W. W.; Kuipers, B. A qualitative method to construct phase portraits. *Eleventh National Conference on Artificial Intelligence*, **1993**.

35. Kuipers, B. *Qualitative Reasoning: Modeling and Simulation with Incomplete Knowledge*; MIT Press, 1994.

36. Bernard, O.; Gouzé, J.-L. Transient behavior of biological loop models, with application to the Droop model. *Mathematical Biosciences* **1995**, *127* (1), 19–43.

37. Show, K.-Y.; Wang, Y.; Foong, S.-F.; Tay, J.-H. Accelerated start-up and enhanced granulation in upflow anaerobic sludge blanket reactors. *Water Research* **2004**, *38*, 2293–2304.

38. Puñal, A.; Trevisan, M.; Rozzi, A.; Lema, J. Influence of C:N rato on the start-up of up-flow anaerobic filter reactors. *Water Research* **2000**, *9*, 2614–2619.

39. Michaud, S.; Bernet, N.; Buffière, P.; Roustan, M.; Moletta, R. Methane yield as a monitoring parameter for the strat-up of anaerobic fixed film reactors. *Water Research* **2002**, *36*, 1385–1391.

40. Cresson, R.; Escudié, R.; Carrère, H.; Delgenès, J.-P.; Bernet, N. Influence of hydrodynamic conditions on the start-up of methanogenic inverse turbulent bed reactors. *Water Research* **2007**, *41*, 603–612.

41. Cresson, R.; Carrère, H.; Delgenès, J.-P.; Bernet, N. Biofilm formation during the start-up period of an anaerobic biofilm reactor - Impact of the nutrient complementation. *Biochemical Engineering Journal* **2006**, *30*, 55–62.

42. Ince, O.; Anderson, G. K.; Kasapgil, B. Control of organic loading rate using the specific methanogenic activity test during start-up of an anaerobic digestion system. *Water Research* **1995**, *29* (1), 349–355.

43. Michaud, S.; Bernet, N.; Buffière, P.; Delgenès, J.-P. Use of the methane yield to indicate the metabolic behaviour of methanogenic biofilms. *Process Biochemistry* **2005**, *40*, 2751–2755.

44. Steyer, J.-P.; Bouvier, J. C.; Conte, T.; Gras, P.; Sousbie, P. Evaluation of a four year experience with a fully instrumented anaerobic digestion process. *Water Science and Technology* **2002**, *45* (4-5), 495–502.

45. Chachuat, B.; Bernard, O. Probabilistic observers for mass-balance based bioprocess models. *International Journal of Robust and Nonlinear Control* **2005**, *16* (3), 157–171.

46. Moisan, M.; Bernard, O.; Gouzé, J.-L. Near optimal interval observers bundle for uncertain bioreactors. *Automatica* **to appear**.